ChemPubSoc Europe

DOI: 10.1002/cplu.201900504

CHEMPLUSCHEM Full Papers

Copper(II) Coordination Abilities of the Tau Protein's N-Terminus Peptide Fragments: A Combined Potentiometric, Spectroscopic and Mass Spectrometric Study

Márton Lukács,[a] Györgyi Szunyog,[a] Ágnes Grenács,[a] Norbert Lihi,[a, b] Csilla Kállay,[a] Giuseppe Di Natale,[c] Tiziana Campagna,[c] Valeria Lanza,[c] Giovanni Tabbi,[c] Giuseppe Pappalardo,[c] Imre Sóvágó,[a] and Katalin Várnagy*[a]

Copper(II) complexes of the N-terminal peptide fragments of tau protein have been studied by potentiometric and various spectroscopic techniques (UV-vis, CD, ESR and ESI-MS). The octapeptide Tau(9-16) (Ac–EVMEDHAG–NH_2) contains the H14 residue of the native protein, while Tau(26-33) (Ac–QGGYTMHQ–NH_2) and its mutants Tau(Q26K-Q33K) (Ac–KGGYTMHK–NH_2) and Tau(Q26K-Y29A-Q33K) (Ac–KGGATMHK–NH_2) include the H32 residue. To compare the binding ability of H14 and H32 in a single molecule the decapeptide Ac–EDHAGTMHQD–NH_2 (Tau(12-16)(30-34)) has also been synthesized and studied. The histidyl residue is the primary metal binding site for metal ions in all the peptide models studied. In the case of Tau(9-16) the side chain carboxylate functions enhance the stability of the M–N_{im} coordinated complexes compared to Tau(26-33) (logK(Cu–N_{im}) = 5.04 and 3.78, respectively). Deprotonation and metal ion coordination of amide groups occur around the physiological pH range for copper(II). The formation of the imidazole- and amide-coordinated species changes the metal ion preference and the complexes formed with the peptides containing the H32 residue predominate over those of H14 at physiological pH values (90%–10%) and in alkaline samples (96%–4%).

Introduction

Tau protein is an intrinsically disordered large protein consisting of 441 amino acids including 12 histidyl residues as potential metal binding sites.[1] The biological role of tau protein is associated with its interaction with tubulins to promote their assembly into microtubules and to stabilize the microtubules.[2,3] Many recent studies suggest that in addition to amyloid-β, tau protein may also play a significant role in the development of Alzheimer's disease and/or other neurodegenerative disorders.[4,5] The neuropathological hallmarks of these diseases are related to the accumulation of amyloid-β into senile plaques and of hyperphosphorylated tau into neurofibrillary tangles.[6,7] Moreover, huge number of recent publications support that metal ions also play a crucial role in neurodegeneration.[8] The interactions of metal ions with prion protein and its peptide fragments and with amyloid-β peptide have been extensively studied and the most important results are summarized in several reviews.[9–16] On the contrary, the association of metal ions with tau protein and its various peptide fragments are much less studied and the results are partly contradictory. It is widely accepted that the aggregation and toxic deposition of tau protein is triggered by hyperphosphorylation of the peptide and this process is significantly influenced by various metal ions.[17] The extent of aggregation of the protein is affected by the concentration and also by the oxidation state of the metal ions[18–20] and the role of the copper or iron catalyzed redox reactions has also been reported.[21] These previous studies strongly support the involvement of metal ions in the formation of neurofibrillary tangles but the exact characterization of the metal binding sites has not been satisfactorily clarified.[8,22]

Imidazole-N donors of histidine are effective metal binding sites of proteins[23,24] and tau protein is relatively rich in this residue. Tau protein sequence also shows some methionine residues especially in the N-terminal domain. These amino acids are, however, rather far from each other in the sequence of the protein and, as a consequence, any of them may be considered as a potential binding site. On the other hand, the microtubule-binding region of tau contains three or four pseudorepeats, each of them has 31–32 amino acid residues including a highly conservative octadecapeptide domain which begins with valine and ends with the PGGG sequence but involves also histidine. The influence of copper(II) ions on the aggregation processes of several fragments from this domain of the protein has already been studied but the exact nature of the metal binding modes

[a] M. Lukács, G. Szunyog, Dr. Á. Grenács, Dr. N. Lihi, Dr. C. Kállay, Prof. I. Sóvágó, Prof. K. Várnagy
Department of Inorganic and Analytical Chemistry
University of Debrecen
Egyetem tér 1, H-4032 Debrecen (Hungary)
E-mail: varnagy.katalin@science.unideb.hu

[b] Dr. N. Lihi
MTA-DE Redox and Homogeneous Catalytic Reaction Mechanisms Research Group
University of Debrecen
Egyetem tér 1, H-4032 Debrecen (Hungary)

[c] Dr. G. Di Natale, T. Campagna, Dr. V. Lanza, Dr. G. Tabbi, Dr. G. Pappalardo
CNR-Istituto di Cristallografia (IC), s.s. Catania
Via Paolo Gaifami 18., 95126 Catania (Italy)

Supporting information for this article is available on the WWW under https://doi.org/10.1002/cplu.201900504

©2019 The Authors. Published by Wiley-VCH Verlag GmbH & Co. KGaA. This is an open access article under the terms of the Creative Commons Attribution License, which permits use, distribution and reproduction in any medium, provided the original work is properly cited.

© 2019 The Authors. Published by Wiley-VCH Verlag GmbH & Co. KGaA

has not been elucidated.[25–27] Saxena et al. used ESR spectroscopy to investigate a series of peptides from this domain and a high similarity in the binding modes of the octadecapeptides has been suggested with involvement of imidazole-N and the backbone amide-N in copper binding.[28]

In almost all previous complexation studies the peptide fragments of the microtubule-binding domain were investigated, although histidines are also present in the N-terminal region of the protein. Moreover, a comprehensive mass spectrometry screening on cerebrospinal fluid samples of patients with Alzheimer disease revealed an increased level of peptide fragments from the N-terminal region.[29] This observation promoted a recent circular dichroism and ESI-MS study on the copper(II) complexes of two peptides encompassing the 1–25 and 26–44 residues of human tau protein.[30] This study undoubtedly proved that the N-terminal domain of tau protein can also effectively bind copper(II) ions and the terminal amino and/or histidyl imidazole nitrogen atoms were suggested as the primary metal binding sites. This paper gave also useful indication about the stoichiometry of the copper(II) complexes. On the other hand, the complete metal complex speciation by potentiometry was not attempted because of the complexity of the system (many pK values in overlapping processes may prevent obtaining of reliable stability constant values) and potential solubility problems of the copper(II) complexes.

In the present paper we selected the putative metal binding site of each peptide and carried out the potentiometric measurements for reliable stability constant values. These values would be useful for the subsequent studies using the longer parent peptides. We report the results of a comprehensive study on the copper(II) complexes of two peptide fragments and their various mutants from the N-terminal region of human tau protein. The octapeptide Tau(9-16) (Ac–EVMEDHAG–NH_2) contains H14 residue of the native protein. Another octapeptide Tau(26-33) (Ac–QGGYTMHQ–NH_2) provide information on the binding ability of H32 residue of the native protein. The solubility of this peptide is rather low in aqueous media thus the glutamine/lysine mutant has also been synthesized and studied (Tau(Q26K-Q33K), Ac–KGGYTMHK–NH_2). The understanding of the observed differences in the metal binding ability of Tau(9-16) and Tau(26-33) made also necessary the synthesis of a Tyr/Ala mutant (Tau (Q26K-Y29A-Q33K), Ac–KGGYTMHK–NH_2). Finally, to compare the binding ability of H14 and H32 in a single molecule, a model decapeptide Tau(12-16)(30-34) (Ac–EDHAGTMHQD–NH_2) has also been synthesized and studied.

Results and Discussion

Protonation Equilibria of the Peptides

Protonation constants of the peptides have been determined by potentiometric measurements and the data are listed in Table 1. It is clear from the Table that the number of the protonation sites is different for each ligand and their charges are also varying depending on the number of carboxylate functions. In general, the deprotonation steps generally significantly overlap thus making difficult the exact assignment of the p*K* values to specific side chains. Comparison of these values with the p*K* values of previously studied peptides, however, provides a good estimation for this question. In the case of Tau (9-16) the imidazole of histidine is the most basic site, while the deprotonations of the carboxylic groups of glutamyl and aspartyl residues occur in the slightly acidic pH range. The *pK* values for the histidyl residue of terminally protected peptides[31] are generally lower than that of Tau(9-16) but the small shift towards the alkaline region can be easily explained by the negative charges of the three carboxylate groups. The p*K* values of Tau(26-33) have been determined in very diluted samples because of the low solubility of the ligand but it is evident that the highest p*K* value belongs to the tyrosyl phenolic-OH. The mutant with two lysyl residues (Ac–KGGYTMHK–NH_2) has four protonation sites and the lysyl amino groups are the most basic sites. Similar observation is obtained for the Tyr/Ala mutant but the absence of the phenolate group results in a slightly increased difference in the basicities of the two amino groups of lysines. The decapeptide Ac–EDHAGTMHQD–NH_2 has five protonation sites and the highest two values belong to the 2 histidyl residues. It can also be observed that the presence of two histidines slightly increases the acidity of the carboxylic functions, while the basicity of imidazole increases as compared to other 2-histidine peptides.[32] All the peptide ligands were also screened for pH dependent conformational changes. To do this, far UV-CD spectra of the free peptides were recorded at pH 7.0 and 10.0 (4–10 pH range) and a selection of these spectra are shown in Figure S1 in the Supporting Information. Peptide conformation

Table 1. Protonation constants of the peptides (T = 298 K, I = 0.2 M).

Species	Tau[9-16] [Ac–EVMEDHAG–NH_2]	Tau[26-33] [Ac–QGGYTMHQ–NH_2]	Tau[Q26K-Q33K] [Ac–KGGYTMHK–NH_2]	Tau[Q26K-Y29A-Q33K] [Ac–KGGATMHK–NH_2]	Tau[10-14][30-34] [Ac–EDHAGTMHQD–NH_2]
[HL]	6.70(1)	9.48(5)	10.71(3)	10.77(1)	7.12(1)
[H_2L]	11.38(2)	15.50(10)	20.84(2)	20.70(2)	13.39(1)
[H_3L]	15.52(2)	–	30.22(4)	26.88(2)	17.87(2)
[H_4L]	18.93(4)	–	36.44(4)	–	21.72(2)
[H_5L]	–	–	–	–	24.93(4)
pK_1	6.70	9.48	10.71	10.77	7.12
pK_2	4.68	6.02	10.13	9.93	6.27
pK_3	4.14	–	9.38	6.18	4.48
pK_4	3.41	–	6.22	–	3.85
pK_5	–	–	–	–	3.21

© 2019 The Authors. Published by Wiley-VCH Verlag GmbH & Co. KGaA

Table 2. Stability constants and spectral data of the copper(II) complexes of the octapeptide Tau(9-16) (T = 298 K, I = 0.2 M KCl).

Species	Log β_{pqr}	Visible spectra λ_{max} [nm] [ε [$M^{-1}cm^{-1}$]]	CD spectra λ_{max} [nm] [Δε [$M^{-1}cm^{-1}$]]	ESR $g_{\|\|}$	$A_{\|\|}$ [$10^4 \times cm^{-1}$]
[CuHL]	9.66(17)	–	–	2.344	148
$[CuL]^-$	5.04(7)	747 (38) (wide)	–	2.315	160
$[CuH_{-2}L]^{3-}$	−8.09(7)	616 (74)	651(+0.34) 557(+0.40) 339(−0.23) 246(+7.13)	2.239	163
$[CuH_{-3}L]^{4-}$	−16.61(11)	530 (144)	627(+1.05) 498(−1.21) 329(+1.20) 295(−0.97) 260(+7.39)	2.194	200
log K(Cu–N_{im})	5.04				
pK_{12}(amide)	6.57				
pK_3(amide)	8.52				

was slightly affected by the different pH values as demonstrated by a strong negative ellipticity observed at 200 nm in all cases. This suggests that the peptide fragments always adopt a disordered structure in solution.

Copper(II) Complexes of the Tau(9-16) Fragment

Stability constants of the copper(II) complexes were obtained from the computer evaluation of potentiometric titrations and the data are collected in Table 2 together with the UV-vis, CD and ESR spectral parameters of the major species.

Figure 1 shows the metal ion speciation of the -copper (II)–Tau(9-16) system.

Both thermodynamic and spectral data reveal a good agreement in the complex formation processes of Tau(9-16) and other terminally protected peptides containing one internal histidyl residue, e.g. the various peptide fragments of prion protein outside the octarepeat domain.[20,22] According to the spectral data, the first two species ([CuHL] and $[CuL]^-$) correspond to the coordination of the imidazole side chain but the equilibrium constant calculated for the Cu–N_{im} binding is slightly higher than the values obtained for the various prion fragments. The stability constants for a simple imidazole coordination is generally around log $K = 4.0 \pm 0.2$.[34] The stability enhancement of Tau(9-16) peptide can be easily explained by the contribution of the side chain carboxylate functions of the aspartyl and/or glutamyl residues. ESR spectra of copper(II)–Tau(9-16) system in the 5–6.5 pH range showed the presence of two different species (Figure S2 in the Supporting Information). The spectrum at pH 6.2 was satisfactorily simulated by using two set of Hamiltonian parameters. The first parameter set ($g_{||} = 2.344$, $A_{||} = 148 \times 10^{-4}\ cm^{-1}$) can be assigned to the [CuHL] species and it is consistent with a histidine nitrogen atom coordinating copper(II) ion.[35] In addition, the lowering of the g-value and the rising of the A-value is a reliable suggestion for coordinating carboxylate which assists histidine moiety ($[CuL]^-$ species).[36]

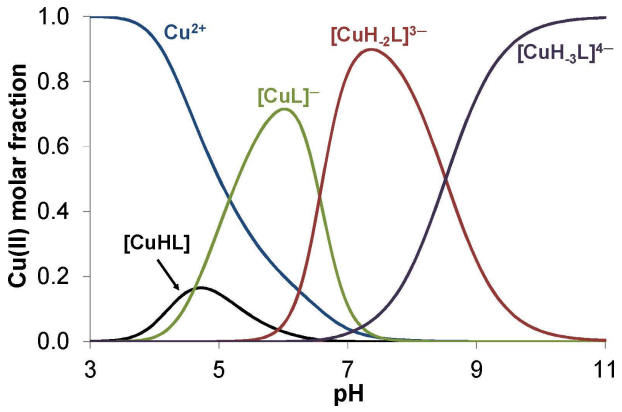

Figure 1. Concentration distribution curves of the major species formed in the copper(II)–Tau(9-16) system (c(L) = c(Cu^{2+}) = 1 mM).

It is also a common feature of the one-histidine peptides that the deprotonation of the first two amide residues takes place in a cooperative process resulting in the (N_{im},N^-,N^-) coordination mode of $[CuH_{-2}L]^{3-}$ which is the dominating species in the physiological pH range. This N_3O coordination environment, corresponding to $[CuH_{-2}L]^{3-}$ species, is also inferred by Hamiltonian parameters drawn from ESR spectra run in the 7–8.5 pH range, i.e. $g_{||} = 2.239$, $A_{||} = 163 \times 10^{-4}\ cm^{-1}$ (Table 2). $[CuH_{-3}L]^{4-}$ is formed in the alkaline samples and its spectral and thermodynamic parameters are very similar to those of other 4 N copper(II) complexes with (N_{im},N^-,N^-,N^-) coordination mode.[31,33–34] The ESR parameters of $[CuH_{-3}L]^{4-}$ species are assigned to a four-nitrogen in plane, although an higher absolute value of $A_{||}$ would have been expected. The value obtained can be explained by considering a small deviation of the coordinating atoms from the planarity, which is also supported by the fairly high ε value for this species (Table 2).

The addition of two equivalents of copper(II) to Tau(9-16) produce little precipitation phenomena as the pH was raised to mild acidic values. ESR spectra at pH values lower than 7 showed mainly the features of copper(II) hexaaqua ion. Starting from pH 7.6 the same parameters for the $[CuH_{-2}L]^{3-}$ species described for 1:1 Cu(II)–Tau(9-16) system were recorded. It is clear that Tau(9-16) can coordinate one metal ion only,

© 2019 The Authors. Published by Wiley-VCH Verlag GmbH & Co. KGaA

Table 3. Stability constants of the copper(II) complexes of Tau(26-33) and its mutants (T = 298 K, I = 0.2 M KCl).

Species	Tau[26-33] [Ac–QGGYTMHQ–NH_2]	Tau[Q26K-Q33K] [Ac–KGGYTMHK–NH_2]	Tau[Q26K-Y29A-Q33K] [Ac–KGGATMHK–NH_2]
[CuH_3L]	–	34.15(3)	–
[CuH_2L]	–	–	25.18(3)
[CuHL]	13.26(14)	23.98(9)	–
[CuL]	–	16.01(2)	14.77(2)
[$CuH_{-1}L$]	3.23(5)	6.68(2)	6.78(3)
[$CuH_{-2}L$]	−5.60(9)	−3.58(2)	−3.19(4)
[$CuH_{-3}L$]	−15.47(8)	−14.09(1)	−13.67(4)
log K(Cu–N_{im})	3.78	3.93	4.48
pK_{12}(amide)	5.01	5.09	5.21
pK_3(amide)	8.83	7.97	7.99
pK(Tyr–OH)	9.87	9.33	–
pK(LysNH_3^+)	–	10.26	9.97
pK(LysNH_3^+)	–	10.51	10.48

although a little clue of a weak site can be seen from the ESR spectrum obtained at pH 7.6. Beside the ESR parameters corresponding the $[CuH_{-2}L]^{3-}$ species, a careful simulation of this spectrum (Figure S3 in the Supporting Information) gave Hamiltonian parameters ($g_{||} = 2.279$, $A_{||} = 179 \times 10^{-4}$ cm^{-1}) similar to those found for another histidine containing peptide coordinating by imidazole nitrogen and amide nitrogen atoms with the involvement of a carboxylate moiety.[37]

Copper(II) Complexes of Tau(26-33) and Related Peptides

Stability constants of the copper(II) complexes of the octapeptides Tau(26-33) and its Gln/Lys and Tyr/Ala mutants are included in Table 3.

The speciation curves for the Gln/Lys mutant (Ac–KGGYTMHK–NH_2) are shown by Figure 2. The corresponding concentration distribution diagrams of the other two peptide complexes are included in the Supporting Information (Figures S4 and S5). At the first sight, the comparison of Figure 1 with Figure 2 (or with Figures S4 or S5) suggests a high complexity in the complex formation processes of the (26-33) mutants.

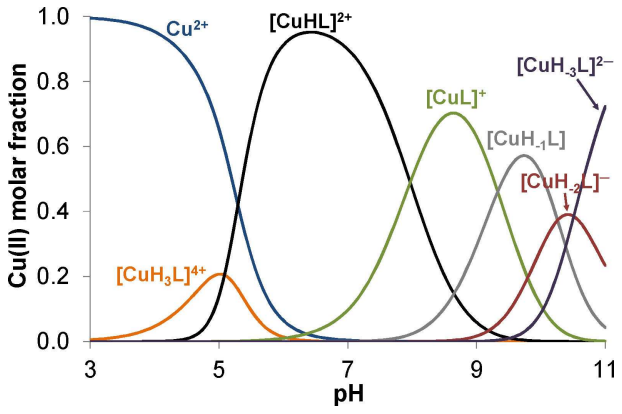

Figure 2. Concentration distribution curves of the major species formed in the copper(II)–Ac–KGGYTMHK–NH_2 system (c(L) = c(Cu^{2+}) = 1 mM).

This is, however, misleading because the high number of different stoichiometries in the alkaline pH range comes from the deprotonation of the non-coordinated lysyl and/or tyrosyl residues. These side chains are generally not metal binding sites in peptide complexes if other strongly coordinating groups (like histidine) are also present in the molecules.[23] As a consequence, the stoichiometry of the same coordination modes can be different due to the presence or absence of the Lys and/or Tyr residues. For example, the Cu–N_{im} coordination mode corresponds to three different stoichiometries, CuH_3L, CuH_2L and CuHL for Ac–KGGYTMHK–NH_2, Ac–KGGATMHK–NH_2 and Ac–QGGYTMHK–NH_2, respectively. Taking into account this effect of the tyrosyl and lysyl residues the number of the major species is the same for the Tau(9-16) and Tau(26-33) fragments. The overall stability of the complexes and especially their spectral characteristics are, however, significantly different suggesting important differences in the metal binding ability and binding modes of the various fragments. All spectroscopic data for the major species of the copper(II)–Tau(26-33) and related systems are included in Table S1 in the Supporting Information.

Thermodynamic and spectroscopic data unambiguously prove that imidazole-N donor atoms are the primary or anchoring sites in all peptide complexes. The stability constants of the corresponding species are around 4.0 log units (see Table 3) which corresponds well the literature data,[34] but much smaller than it was obtained for the Tau(9-16) fragment (Table 2), due to the absence of the negatively charged carboxylate functions.

Deprotonation and coordination of the first two amide groups takes place in a cooperative manner resulting in the formation of the (N_{im},N^-,N^-) coordination mode.

This process was observed for the Tau(9-16) fragment in analogy to many other peptides containing internal histidyl residues. However the thermodynamic and spectral data of Tau (26-33) and its mutants are significantly different from those of Tau(9-16). The pK values for the amide deprotonation are significantly lower for the Tau(26-33) complexes suggesting an extra-stabilization in the corresponding species.

ESR spectra run on frozen solutions of Cu(II)–Tau(26-33) and Cu(II)–Tau(Q26K-Q33K) systems at pH around neutrality gave

© 2019 The Authors. Published by Wiley-VCH Verlag GmbH & Co. KGaA

Hamiltonian parameters in agreement with the three-nitrogen coordination for [$CuH_{-1}L$] and [CuHL] species (Figure S6 in the Supporting Information). These values are $g_{||}=2.214$, $A_{||}=191\times10^{-4}\,cm^{-1}$ and $g_{||}=2.221$, $A_{||}=191\times10^{-4}\,cm^{-1}$ for -Cu (II)–Tau(26-33) and Cu(II)–Tau(Q26K-Q33K) systems, respectively. The $A_{||}$ value obtained for both systems at neutral pH is higher than would be expected for an N_3O coordination environment. Additional information comes from d-d band wavelength (590 nm for both species) which is blue-shifted of about 20 nm than expected for a (N_{im},N^-,N^-) coordination mode. A wide range of studies carried out on Cu(II) binding to a variety of oligopeptides containing methionine residues revealed the possibility of S→Cu(II) interactions and distinct band for CD spectra in the region 320–330 nm can be observed. Indeed starting from moderate acidic pH a charge transfer (CT) band at about 330 nm is visible in the CD spectra, but it results to be embedded in the CT band of coordinating amides at neutral pH (328 nm). On the light of these clues, involvement of the sulphur methionine atom in the coordination plane can be inferred.[38] As the pH is brought to alkaline values an additional amide nitrogen atom deprotonates and replaces the sulphur atom (N_{im},N^-,N^-,N^-). This coordination environment change causes a strong blue-shift of the d-d band wavelength, the lowering of the $g_{||}$-values as well as a significant increment of the absolute $A_{||}$-values (Table S1).

The enhanced stability of the (N_{im},N^-,N^-) coordination mode in the Cu(II)–Tau(26-33) system was supported by far-UV CD investigations. In particular, the far-UV CD spectra of Tau peptides are characterised by a strong negative band below $\lambda=200$ nm, typical of peptides in a random-coil conformation (Figure S1). The reduction of the negative ellipticity centred below $\lambda=200$ nm in the presence of equimolar copper(II) ion, suggests a structuring effect of the metal ion within the polypeptide backbone (Figure S7) as a function of the increasing pH value. A clearer evidence of the metal induced conformational changes is provided by subtracting the apopeptide CD curve profile at the same pH value from the corresponding CD spectra obtained in the presence of -copper (II). The resulting difference CD spectra profile of the Cu(II)–-Tau (26-33) system reveals the appearance of a positive band centred around $\lambda=190$–200 nm and a negative band centred around $\lambda=210$–220 nm at pH 7 (Figure S7a). This well-defined CD-curve profile has been already reported in our previous works and is indicative of conformational changes mainly related to the copper(II) coordination by imidazole side chain of histidine residue and the amide nitrogens.[27] Interestingly, the different far-UV CD spectra of the Cu(II)–Tau(26-33) system reveal the appearance of this distinctive CD band profile at lower pH (pH 5–6) than those reported in the Cu(II)–Tau(9-16) system thereby suggesting an enhanced stability of the (N_{im},N^-,N^-) coordination mode in the former metal-peptide system.

The spectral parameters of the Tau(26-33) fragment and its Gln/Lys and Tyr/Ala mutants are rather similar to each other and this also holds for thermodynamic data if the different numbers of the non-coordinated side chains are taken into account. This observation strongly supports that neither lysyl nor tyrosyl residues take part in metal ion coordination. The aforementioned spectral evidence strongly supports that extra-stabilization of the copper(II) complexes of Tau(26-33) fragments comes from the different binding mode of the complexes. Figure 3 shows the speciation of a model system in which the copper(II) ion and the peptides Tau(9-16) and the Lys mutated Tau(26-33) are present in equimolar concentrations. It is clear from this Figure that there is slight preference for binding to His14 in slightly acidic media. The involvement of the (N_{im},N^-,N^-,S_{met}) donor atoms in copper binding, however, reverses this tendency and His32 becomes the primary binding site of the peptide in neutral and alkaline samples.

Copper(II) Complexes of the Decapeptide Ac–EDHAGTMHQD–NH_2

The potentiometric and spectroscopic results obtained for the binary complexes revealed that copper(II) binding to the peptide fragments including His32 residue is favoured over His14. This conclusion was, however, obtained from measurements performed with small peptides containing only one histidine, while the protein contains all possible metal binding sites. A good model for the comparison of the metal binding ability can be obtained if the specific sequences around His14 and His32 sites are connected in one terminally protected peptide molecule. The decapeptide Ac–EDHAGTMHQD–NH_2 has been synthesized and it contains the 12–16 residues (EDHAG) linked to the 30–34 residues (TMHQD). The equilibrium data and spectroscopic parameters of the decapeptide are included in Table 4. The corresponding speciation curves are plotted in Figures 4.a and 4.b at 1:1 and 2:1 metal to ligand ratios, respectively.

pH-dependent CD spectra of the 1:1 system (see Figure S8 in the Supporting Information) reveal that amide coordinated species are not formed below pH 6.0. As a consequence, the imidazole-N and carboxylate-O donors are the possible binding sites in the complexes $[CuH_2L]^{2+}$, $[CuHL]^+$ and [CuL]. The protonated species are present in rather low concentration and

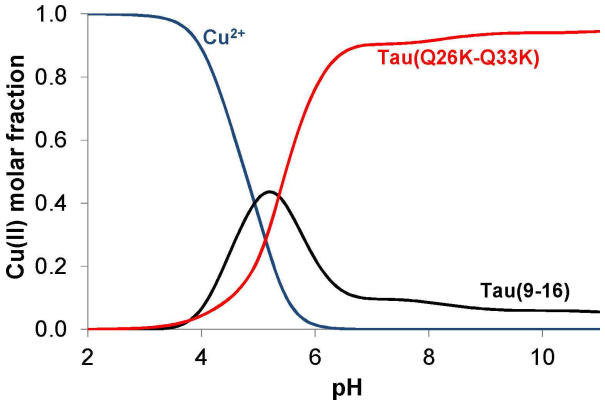

Figure 3. Concentration distribution of copper(II) ion in a model system containing copper(II) and the peptides Tau(9-16) and Tau(Q26K-Q33K) mutants in equimolar concentration (c = 1 mM).

© 2019 The Authors. Published by Wiley-VCH Verlag GmbH & Co. KGaA

Table 4. Stability constants ($\log\beta_{pqr}$) and spectral data of the complexes formed in the copper(II)–Ac–EDHAGTMHQD–NH_2 system (T = 298 K, I = 0.2 M KCl).

Species	log β_{pqr}	Visible spectra $\lambda_{max}[\varepsilon]$	CD spectra $\lambda_{max}[\Delta\varepsilon]$	ESR spectra $g_{\|\|}$	ESR spectra $A_{\|\|}$ [$10^4\times cm^{-1}$]
M/L 1:1					
$[CuH_2L]^{2+}$	16.77(5)	–	–	–	–
$[CuHL]^{+}$	12.24(6)	–	–	–	–
[CuL]	7.66(3)	–	–	2.295	176
$[CuH_{-2}L]^{3-}$	−5.75(5)	590(75)	620 (−0.40) 504 (+0.08) 331 (+0.61) 297 (−0.15) 255 (+2.89)	2.217	195
$[CuH_{-3}L]^{4-}$	−14.21(9)	564(90)	663 (+0.22) 567 (−0.62) 496 (+0.28) 357 (−0.02) 279 (+2.57)	2.204	208
M/L 2:1					
$[Cu_2H_{-3}L]^{2-}$	−7.18(5)	–	–	–	–
$[Cu_2H_{-4}L]^{3-}$	−14.38(11)	–	–	2.219	186
$[Cu_2H_{-5}L]^{4-}$	−22.67(15)	–	–	2.228	183
$[Cu_2H_{-6}L]^{5-}$	−32.12(15)	550(86)	642 (+0.49) 546 (−0.51) 492 (−0.43) 367 (−0.03) 308 (+0.96) 266 (+3.17)	2.196	204
log *K* (Cu–$2N_{im}$)	7.66				
pK_{12}(amide)	6.71				
pK_3(amide)	8.47				

it rules out the exact assignment of the binding sites. [CuL] is the major species between pH 5–7 and its stoichiometry strongly supports the involvement of both imidazole moieties in copper(II) binding. The stability constant is, however, significantly higher than those reported for other $2N_{im}$ coordinated complexes, which are generally around 5–6 log units. The value (log K = 7.66) in Table 4 unambiguously indicates that the carboxylate residues also contribute to the metal binding in this species. Further confirmation for this coordination environment comes from the ESR spectrum at pH 5.8 showing a minor percentage of $[CuH_{-2}L]^{2-}$ (which was subtracted from the spectrum) and the main [CuL] features, characterized by $g_{||}$ = 2.295, $A_{||} = 176\times10^{-4}$ cm^{-1} which are typical of a chromophore formed by two imidazole nitrogen atoms and a deprotonated carboxylate as previously reported.[40,41]

Deprotonation and metal ion coordination of the first two amide groups occur in a cooperative process resulting in the formation of $[CuH_{-2}L]^{2-}$. The protonation constant for this reaction is pK_{12} = 6.71, while 6.57 and 5.01 were obtained for the same process with the Tau(9-16) and Tau(26-33) fragments, respectively (see Tables 2 and 3). These data may support the preference of copper(II) binding to the histidine close to the amino terminus (modelling the His14 residue) but the comparison of CD parameters led to the opposite conclusion (see Table 4 and Table S1).

This dichotomy can be resolved if one takes into account the effect of the macrochelation of the two histidines. The enhanced stability of the [CuL] shifts the coordination of the amide groups into a higher pH range but the preference for copper(II) binding to His32 above pH 7.0 remains intact. Of course, two coordination isomers of $[CuH_{-2}L]^{2-}$ can exist in solution in which the coordination start from the His14 or His32 residues but comparison of the UV-vis and CD spectra strongly support that the ratio of the latter binding mode is more than 90%. According to this hypothesis, the far-UV CD spectra of -Tau(12-16)(30-34), were characterised by a strong negative band below λ = 200 nm (Figure S1). Changes upon addition of the metal ion at 1:1 metal to peptide ratio (Figure S9a) were observed showing a reduction of the negative ellipticity at λ = 200 nm at pH 5–6. Interestingly, the different spectra obtained at pH 5 and pH 6 (Figure S9, Inset) appear quite different from those observed in Cu(II)–Tau(9-16) and Cu(II)–Tau(26-33) systems, when the (N_{im},N^-,N^-) binding mode is favoured as suggested by potentiometric and spectroscopic results, revealing a different coordination mode of copper(II). The observed CD profiles are reminiscent of those reported for copper(II) complexes of prion peptide fragments when macrochelate complex species form.[39]

Moreover, the far-UV CD spectra of Cu(II)–Tau(12-16)(30-34), recorded at higher pH values (Figure S9a, pH range 7–10) revealed the presence of a growing negative band around λ = 220 nm and a small positive band centred at λ = 250 nm. Similar variations in the CD-band profiles were also found for the copper(II) complexes of the peptide fragments Tau(26-33) suggesting the preference for copper(II) binding at His32 sites at 1:1 metal to peptide ratio and basic pH values.

All these results are in a good agreement with those obtained for the small one-histidine fragments as it was demonstrated by Figure 4. The Hamiltonian parameters of the $[CuH_{-2}L]^{2-}$ species, obtained from ESR spectrum around physiological pH are very similar to those belonging to Cu(II)–Tau(26-33) and Cu(II)–Tau(Q26K-Q33K) systems at the same pH (Figure S10 in the Supporting Information). Also, the d-d band value is coincident. In other words, a similar scenario in which methionine sulphur atom coordinates Cu(II) in-plane turned out again. Further deprotonation at higher pH values leads to the formation of $[CuH_{-3}L]^{3-}$ species where the amide nitrogen atom replaces methionine coordination. The Hamiltonian parameters are in line with a (N_{im},N^-,N^-,N^-) coordination environment. It is a common feature of multihistidine peptides that all imidazole

© 2019 The Authors. Published by Wiley-VCH Verlag GmbH & Co. KGaA

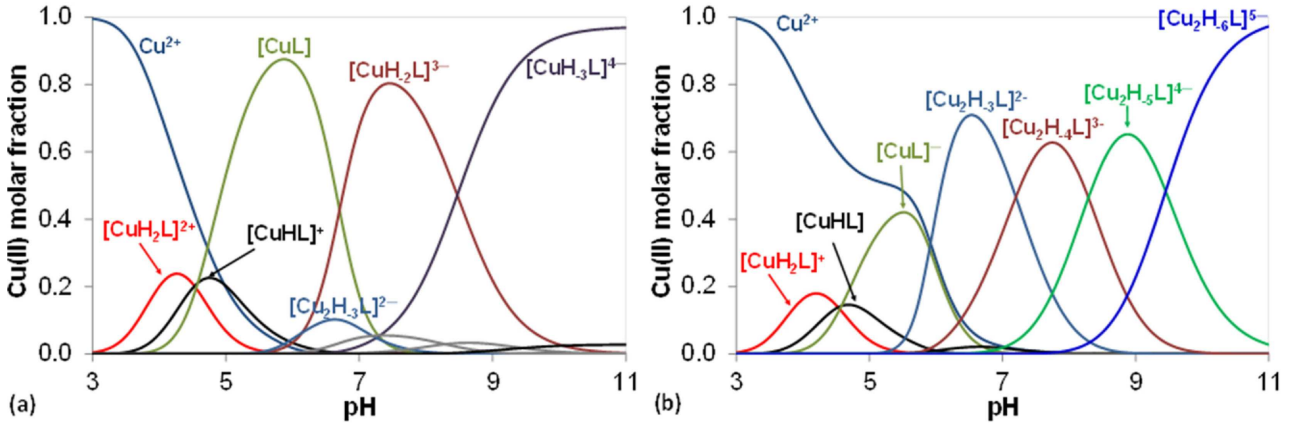

Figure 4. Concentration distribution curves of the major species formed in the copper(II)–Ac–EDHAGTMHQD–NH_2 system, 1:1 ratio (a), 2:1 ratio (b) (c(L) = 1 mM).

side chains can be independent metal binding sites resulting in the formation of polynuclear complexes.[6,32] The potentiometric and spectroscopic measurements performed in the presence of excess metal ion support this expectation and provided direct evidence for the formation of dinuclear complexes with the decapeptide.

Table 4 and Figure 4.b show that the stoichiometry of the dinuclear complexes varying from $[Cu_2H_{-3}L]^-$ to $[Cu_2H_{-6}L]^{4-}$ indicating that the involvement of amide nitrogen donors is crucial for the formation of the dinuclear species. The high complexity of the speciation curves does not allow the determination of the exact spectral parameters for all dinuclear complexes but the analysis of UV-vis, CD, ESR and mass spectra (see below) provides a series of evidence for the existence of dinuclear complexes.

In particular, the far-UV CD spectra of Cu(II)–Tau(12-16)(30-34) at 2:1 metal to peptide ratio (Figure S9b), indicate that the addition of one more equivalent of copper(II), in the pH range 7–10, resulted in a more-intense CD signal at $\lambda = 250$ nm, similar to the CD band observed in the Cu(II)–Tau(9-16) system, suggesting the involvement of the His14 sites in the coordination of the second equivalent of copper(II).

Moreover, the bandwidth of the visible spectra measured for 2:1 system (Figure S11) is higher than it was measured for the one-histidine fragments. This comes from the fact that the absorption maxima of the fully deprotonated species ($[CuH_{-3}L]$) are 530 nm for the Tau(9-16) peptide and around 560 nm for all Tau(26-33) fragments. The corresponding value for the dinuclear complex ($[Cu_2H_{-6}L]^{4-}$) is 550 nm. Figure 5 is used to compare the CD spectra of the above-mentioned species. It is clear that the CD pattern of the dinuclear complex significantly differ from the mononuclear ones but the superposition of these spectra is in a very good agreement with that of the measured spectra of the dinuclear species.

Finally, ESR spectra measured on frozen solutions of -copper (II)–Ac–EDHAGTMHQD–NH_2 system (metal-to-ligand ratio 2:1) showed a coordination of the two copper centers which is very similar to those seen for metal-to-ligand ratio 1:1, as the pH is varied (Figure S12 in the Supporting Information). Of course, it

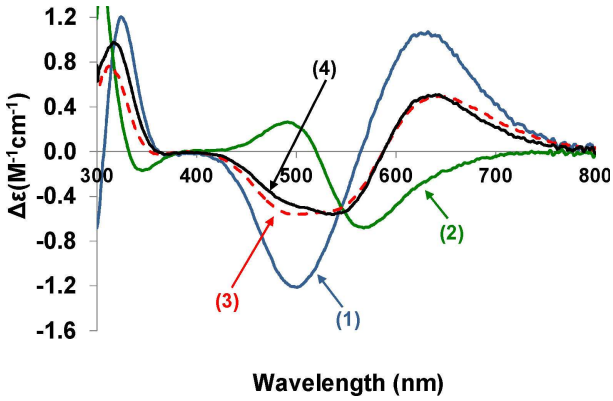

Figure 5. Visible CD spectra of the $[CuH_{-3}L]^{4-}$ complexes of Tau(9-16) (Ac–EVMEDHAG–NH_2) (1), Tau(Q26K-Q33K) (Ac–KGGYTMHK–NH_2) (2), $[Cu_2H_{-6}L]^{4-}$ of Ac–EDHAGTMHQD–NH_2 (3) and superposition of CD spectra of the $[CuH_{-3}L]^{4-}$ complexes of Tau(9-16) and Tau(Q26K-Q33K) in 1:1 ratio (4).

is not possible to distinguish among different isomers and the parameters obtained can be considered as an average of the very similar coordination environments formed at each pH value.

High Resolution ESI-MS Analysis

Fourier Transform (FT-MS) and tandem mass spectrometry investigations provided additional information regarding the copper(II) interaction with Tau peptide fragments. The observation of mononuclear species, at 1:1 metal-to-ligand ratio, suggested the presence of one copper(II) binding site in the Tau(9-16) and Tau(26-33) peptide fragments. Dinuclear species can be also observed in the copper(II)–Tau(12-16)(30-34) system at 2:1 metal to peptide ratio (Figure S13).

HCD (High energy Collision Dissociation) of copper(II) complexes, selected as precursor ions, was used to investigate the metal–peptide interaction. Copper(II) complexes of Tau(9-16), Tau(26-33) and Tau(12-16)(30-34) peptide fragments dis-

© 2019 The Authors. Published by Wiley-VCH Verlag GmbH & Co. KGaA

sociated at CE lower than the respective apo–peptide fragments (Table S2, see Supporting Information for more details). This indicates that a metal ion induces fragmentation of peptide complexes.[42] Comparison of the fragmentation pattern observed in the MS/MS spectra, at collision energies (CE) needed to start the precursor ion fragmentation, of the protonated (Figure 6) and metal-bound peptides (Figure 7), provided interesting information about the amino acid residues involved in the copper(II) coordination. The principal fragments observed in the apo–peptides (Figure 6) were generated by the cleavage of amide bonds distributed along the entire peptide backbone (see supporting information for more details).

On the other hand, HCD of the metal-bound peptides, low collision energy conditions (Figure 7), produced *primarily* the b_n fragments obtained by the cleavage of peptide bond at the C-terminal side of histidine residue. The cleavage of peptide bond that occurred next to the metal–ion binding site was already reported by the others.[43,44] A plausible mechanism was suggested in Scheme S1 (see supporting information for more details). Interestingly, the MS/MS spectra recorded for the -Cu(II)–Tau(12-16)(30-34) system at 1:1 metal to peptide ratio (Figure 7) indicate that the peak corresponding to the Cu-b_9 fragment was the principal fragment observed when the mononuclear complex species started dissociation reaction at CE 40. Therefore, dissociation of the His_{32}–Gln_{33} amide bond is favoured over dissociation of the His_{14}–Ala_{15} bond suggesting the copper(II) preference for binding to the His_{32} binding site. It is important to note that the Cu-b_3 fragment can also be observed in the MS/MS spectra recorded at higher collision energies (CE = 50, Figure 7). Metal ion induced dissociation of the His_{14}–Ala_{15} bond may indicate a coordination mode where both histidine side chains are involved in the copper complexation as suggested by potentiometric results of the Cu(II)–Tau(12-16)(30-34) system at slightly acid pH values. When high CE values are applied, the multi-histidine coordination mode can be disrupted and the fragment formed in these conditions can be rationalized on the basis of competitive binding of Cu(II) between the histidine side chains. The formation of a multi-histidine coordination mode can also justify the higher collision energy needed to start the fragmentation of Cu(II)–Tau(12-16)(30-34) (CE 40) in comparison with CE of Cu(II)–Tau(9-16) (CE 20) or Cu(II)–Tau(26-33) (CE 20) systems (Table S2).

The copper(II) preference for binding to the His_{32} binding site was further supported by the MS/MS spectra of Cu(II)–Tau(9-16) and Cu(II)–Tau(26-33) precursor ions, recorded at high collision energy (CE = 50) (Figure S14). In particular, the comparison of the spectra revealed a different fragmentation pattern suggesting the involvement of Met31 side chain in the metal coordination at the His32 binding (see the Supporting Information for more details).

Conclusion

The studies reported in this manuscript give a comprehensive view on the copper(II) binding ability of the N-terminal domain of tau protein. Octapeptide fragments Tau(9-16) (Ac–EVMEDHAG–NH_2) including the His14 residue of the protein and Tau(26-33) (Ac–QGGYTMHQK–NH_2) including His32 site and some of its mutant have been first synthesized and their copper(II)) complexes studied by the combined application of solution equilibrium and various spectroscopic techniques (UV-vis, CD, ESR, ESI-MS). Both fragments are able to bind copper(II) ions. Histidyl residues are the primary metal binding

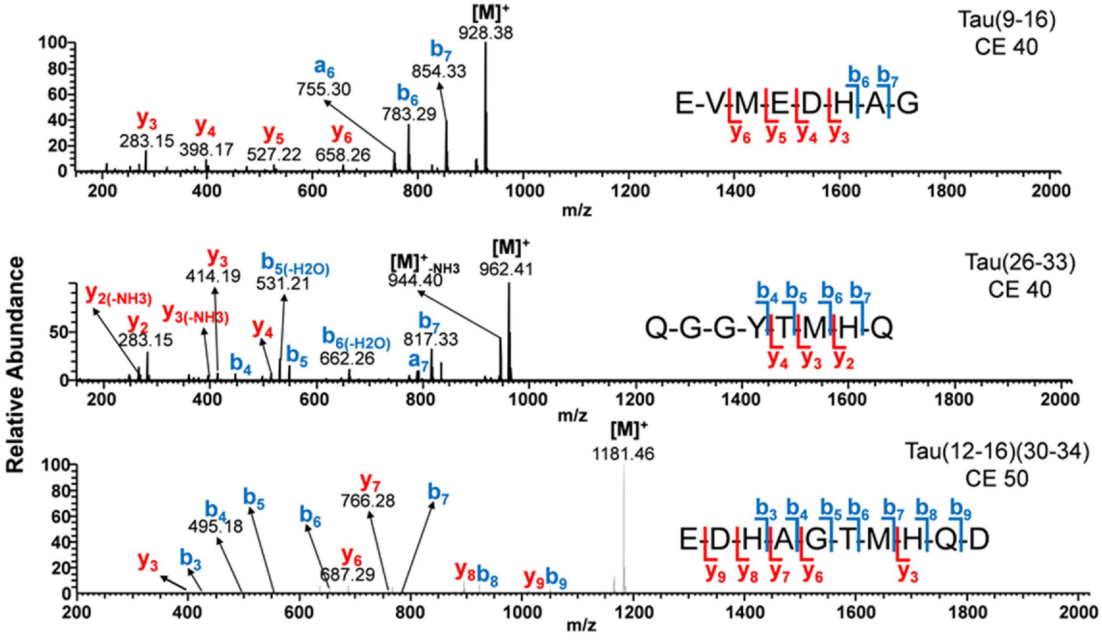

Figure 6. HCD spectra of single-charged peptides Tau(9-16) (m/z $[M]^+ = 928.38$); Tau(26-33) (m/z $[M]^+ = 962.41$) and Tau(12-16)(30-34) (m/z $[M]^+ = 1181.46$). Collision energies (CE) needed to start the precursor ion fragmentation were applied. The b_n/a_n type fragment (blue color) and y_n type fragments (red color) produced through the cleavage of a bond in the peptide chain were also reported for each MS/MS spectrum.

© 2019 The Authors. Published by Wiley-VCH Verlag GmbH & Co. KGaA

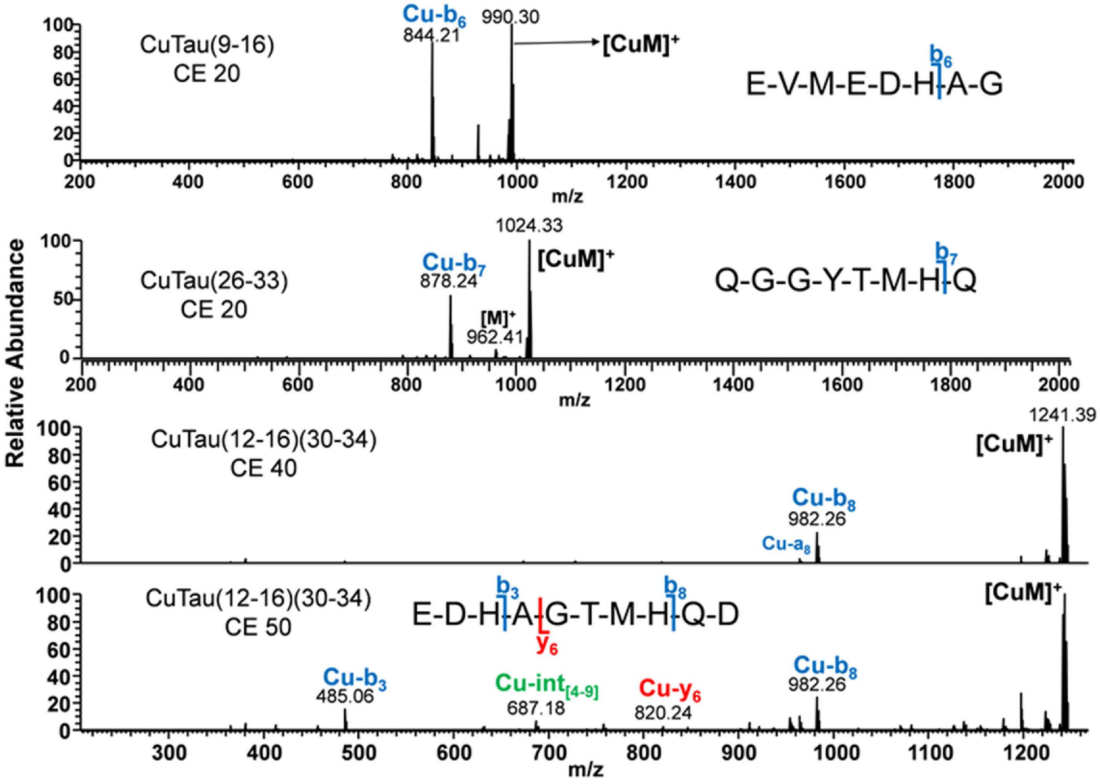

Figure 7. HCD spectra of single-charged copper complexes Cu(II)–Tau(9-16) (m/z $[M]^+ = 990.30$), Cu(II)–Tau(26-33) (m/z $[M]^+ = 1024.33$, Cu(II)–Tau(12-16)(30-34) (m/z $[M]^+ = 1241.39$) at CE 40 and CE 50. Collision energies (CE) needed to start the precursor ion fragmentation were applied. Only the metal bound b_n/a_n type fragment (blue color) and y_n type fragments (red color), produced through the cleavage of a bond in the peptide chain, were indicated. The fragments in green color correspond to an internal fragment.

sites, but in the case of Tau(9-16) the side chain carboxylate functions enhance the stability of the M–N_{im} coordinated complexes. These species are present only in slightly acidic solutions. Increase of pH results in the deprotonation and metal ion coordination of the amide groups preceding the histidyl sites. In the case of copper(II) the deprotonation of the first two amide takes place in a cooperative manner which is a common feature of the terminally protected peptides including internal histidyl residues. This process results in the (N_{im},N^-,N^-) coordination mode and this is the predominating species in the physiological pH range. Deprotonation and copper(II) coordination of the third amide group occurs under slightly alkaline conditions. As a consequence, the donor atoms of the major species in basic solutions are (N_{im},N^-,N^-,N^-). The change of the binding mode from the simple monodentate imidazole binding to the amide bonded complexes changes the metal ion preference of the two histidyl sites, as well. For the latter binding mode His32 site predominates over His14. However, taking into account the different pH ranges for the formation of the corresponding copper(II) complexes His32 is the preferred binding site for copper(II) at the physiological pH. This preference in the metal binding of the histidyl sites remains intact even if the two sequences are combined in a model peptide. The decapeptide Ac–EDHAGTMHQD–NH_2 contains histidines in the same environments as in the native fragments. The CD spectra give an unambiguous proof for the binding of copper(II) to the second histidyl residue in alkaline samples similar to the one-histidine counterpart. There are, however, two major differences in the complex formation processes: the decapeptide can keep two equivalents of copper(II) ions in solution resulting in the formation of dinuclear complexes in which the histidines are independent metal binding sites. It is our opinion that the two imidazoles can form macrochelates enhancing the overall metal binding ability of the decapeptide.

The results presented in this work may contribute to further advance of our knowledge about the metal binding affinities of the less studied N-terminal region of the tau protein.

Experimental Section

Materials

Solvents and chemicals used for synthetic purposes were obtained from commercial sources in the highest available purity and operated without further purification. The Rink Amide AM and NovaSyn TGR resin, all of the N-fluorenylmethoxycarbonyl (Fmoc)-protected amino acids (Fmoc–Gln(Trt)–OH, Fmoc–Asp(OtBu)–OH, Fmoc–Glu(OtBu)–OH, Fmoc–His(Trt)–OH, Fmoc–Lys(Boc)–OH, Fmoc–Met–OH, Fmoc–Thr(tBu)–OH, Fmoc–Tyr(tBu)–OH, Fmoc–Ala–OH, Fmoc–Val–OH Fmoc–Gly–OH) and 2-(1-H-benzotriazol-1-yl)-1,1,3,3-tetramethyluronium tetrafluoroborate (TBTU) were purchased from Novabiochem (Switzerland). 2-methyl-2-butanol, N-hydroxybenzotriazole hydrate (HOBt·H_2O), N-methyl-pyrrolidone

© 2019 The Authors. Published by Wiley-VCH Verlag GmbH & Co. KGaA

(NMP), 2,2′-(ethylenedioxy)diethanethiol (DODT), N,N,N′,N′-Tetramethyl–O-(1H-benzotriazol-1-yl)uronium hexafluorophosphate and triisopropyl-silane (TIS) were purchased from Merck, while N,N-diisopropylethylamine (DIPEA) and trifluoroacetic acid (TFA) were Merck Millipore Co. products. Peptide-synthesis grade N,N-dimethylformamide (DMF) and acetic anhydride (Ac_2O) were bought from VWR International, while piperidine, dichloromethane (DCM), diethyl ether (Et_2O), acetic acid (AcOH) and acetonitrile (ACN) from Molar Chemicals Ltd.

As concerns Cu(II) ions, stock solution ($CuCl_2$) was prepared from analytical grade reagents (Reanal) and its concentration was verified gravimetrically via the precipitation of oxinate.

Peptide Synthesis

In the case of the investigated peptides solid phase peptide synthesis was performed with the aid of a microwave-assisted Liberty Peptide Synthesizer (CEM, Matthews, NC). Fmoc/tBu method and TBTU/HOBt/DIPEA activation strategy were used. Cleaving of α-amino protecting group of amino acids and resin was performed with a 20 V/V% piperidine and 0.1 M $HOBt \cdot H_2O$ in DMF solution at 80 °C with 30 W microwave power for 180 s. Four times excess of amino acids and 30 W microwave power for 300 s were used for coupling at 80 °C in the presence of 0.5 M HOBt and 0.5 M TBTU in DMF as an activator and 2 M DIPEA in NMP as an activator base. The free amino terminus was treated with DMF containing 5 V/V% Ac_2O and 6 V/V% DIPEA to obtain the acetylated amino group. After the finishing of synthesis, peptides were cleaved from their respective resins, with the simultaneous removal of the side chain protective groups, by treatment with a mixture of TFA/TIS/H_2O in 94/2.5/2.5/1 V/V% or TFA/TIS/H_2O 95/2.5/2.5 V/V% for 2 h at room temperature. Each solution containing the free peptide was separated from the resin by filtration. Cold Et_2O was used to precipitate the crude peptides from the solution and to wash from the contaminants of the reagents of the synthesis and cleaving agents. After filtering the product was dried under vacuum, redissolved in water and lyophilized. The schematic structures of the synthesized peptides are shown in Scheme 1.

The purity of the peptides (~90%) was checked by analytical RP-HPLC and ESI-TOF and/or MALDI-TOF MS analysis, while the protonation sites were identified by pH-potentiometric measurements.

The purification of other peptides was carried out by preparative reversed-phase HPLC using a Preparative scale-up LC-20A HPLC-DAD system (Shimadzu) chromatography system with detection at 222 nm. To Ac–QGGYTMHQ–NH_2, Ac–KGGYTMHK–NH_2 and Ac–EDHAGTMHQD–NH_2 Synergi, Fusion-RP C18 250×10 mm (80 Å pore size, 4 μm particle size), to Ac–KGGATMHK–NH_2 Phenomenex, Jupiter Proteo C12 250×4.6 mm (90 Å pore size, 4 mm particle size), column were used. The peptides were eluted at a flow rate of 10 ml/min, where eluent was the mixture of solvent A (H_2O containing 0.1% TFA) and B (CH_3CN containing 0.1% TFA) in different percentage depending on pertinent method.

Potentiometric Measurements

pH-potentiometric titrations were completed on 3.00 mL samples at 1–2 mM total ligand concentration with the aid of carbonate free stock solution of potassium hydroxide of known concentration (approximately 0.2 M). The metal to ligand ratios were selected between 1:1 and 2:1. During titration, argon was bubbled through the sample to ensure the absence of oxygen and carbon dioxide. The samples were stirred using a VELP scientific magnetic stirrer.

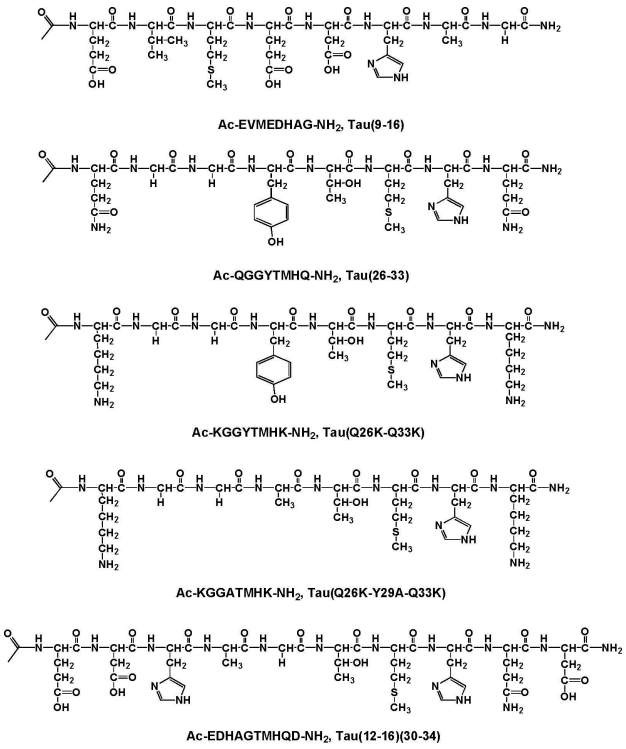

Scheme 1. The structural formulae of peptides.

All pH-potentiometric measurements were carried out at 298 K and at constant ionic strength of 0.2 M KCl. pH measurements were made with a MOLSPIN pH-meter equipped with a 6.0234.100 and 6.0234.110 combination glass electrode (Metrohm) and the titrant was dosed by means of a MOL-ACS burette controlled by a computer. During the titrations the following equilibrium conditions were used: the system is in equilibrium if the maximum change of potential is 0.03 mV for 9 seconds. The recorded pH readings were converted into hydrogen ion concentration as described by Irving et al..[45] Protonation constants of the ligands and overall stability ($\log\beta_{pqr}$) constants of the metal complexes were calculated by means of general computational programs (PSEQUAD[46] and SUPERQUAD[47]) based on the [Equation (1) and (2)].

$$p\ M + q\ H + r\ L \rightleftharpoons M_pH_qL_r \quad (1)$$

$$\beta_{pqr} = \frac{[M_pH_qL_r]}{[M]^p[H]^q[L]^r} \quad (2)$$

UV-Vis Spectroscopy

The same concentration range as used for pH-potentiometry was selected to register the UV-vis spectra of the copper(II) complexes. A Perkin Elmer Lambda 25 scanning spectrophotometer was applied in the wavelength range of 250–900 nm.

Circular Dichroism (CD) Spectroscopy

A JASCO J-810 spectropolarimeter was used to perform the circular dichroism (CD) measurements. CD spectra of the copper(II) complexes were acquired from 220 to 800 nm using 1 cm and

© 2019 The Authors. Published by Wiley-VCH Verlag GmbH & Co. KGaA

1 mm cells and at the same concentration as applied for pH-potentiometric measurements. Far UV-CD spectra were recorded between 190–260 nm and the concentration of the ligand in the sample changed between 0.15–0.20 mM.

Electron Spin Resonance (ESR) Spectroscopy

A Bruker Elexsys E500 CW-ESR spectrometer driven by a PC running XEpr program under Linux and equipped with a Super-X microwave bridge operating at 9.3–9.5 GHz, and a SHQE probe head was used throughout this work. All frozen solution ESR spectra of copper(II) complexes were recorded at 150 K by means of an ER4131VT variable temperature apparatus. Copper(II)-peptide samples were added of a small amount of methanol (up to 10%) in order to increase spectral resolution. Parallel spin Hamiltonian parameters were taken directly from the experimental spectra, always calculating them from the 2nd and 3rd line to get rid of errors coming from second order effects.[48] An improved resolution of the ESR spectra[37] was obtained with the use of isotopically pure $^{63}Cu^{2+}$. In order to achieve a better determination of the magnetic parameters, some of the experimental spectra were simulated by the program Monoclin[50,51] (which is able to discriminate one or more species). Instrumental settings of frozen solution ESR spectra were as follow: number of scans 2–10; microwave frequency 9.433–9.437 GHz; modulation frequency 100 kHz; modulation amplitude 0.7 mT; time constant 163 ms; sweep time 2.8 min; microwave power 20 mW; receiver gain 50–60 dB.

Mass Spectrometry

High-resolution (HR) ESI-MS spectra were recorded using Q Exactive (Orbitrap) mass spectrometer (Thermo Fisher Scientific instruments) in the same concentration range as used for Far-UV CD measurements. Copper(II) complex solutions were introduced into the ESI source on 100 mm internal diameter fused silica via a 500 ml syringe. Full MS scans in the m/z range 200–2000 were acquired with MS resolution of 150.000 FWHM (at m/z 400) in the Orbitrap. Precursor ions of protonated peptides and metal bound peptides at 1:1 metal-to-ligand ratio, were selected for Higher Energy Collisional Dissociation (HCD) at different collision energies (CE). MS/MS scans were acquired in the Orbitrap analyzer at 150.000 FWHM resolution. The experimental conditions for spectra acquired in the positive ion mode were: spray voltage = 3.5 kV, capillary temperature = 250 °C; m/z range = 200–2000, S-lens RF level = 60 V, Sheath gas = 5. The molecular species were detected as clusters of peaks because of the isotopic distribution of elements. The m/z values indicated in the spectra correspond to most abundant ions of each cluster.

Acknowledgements

The research was supported by the EU and co-financed by the European Regional Development Fund under the project GINOP-2.3.2-15-2016-00008, the Hungarian National Research, Development and Innovation Office (NKFIH K115480 and PD-128326) and by the János Bolyai Research Scholarship of the Hungarian Academy of Sciences. The authors are also grateful for the support by the MTA (Hungary) – CNR (Italy) bilateral program.

Conflict of Interest

The authors declare no conflict of interest.

Keywords: binding sites · copper · mass spectrometry · peptides · tau proteins

[1] M. Goedert, M. G. Spillantini, R. Jakes, D. Rutherford, R. A. Crowther, *Neuron* **1989**, *3*, 519–526.
[2] D. W. Cleveland, S.-Y Hwo, M. W. Kirschner, *J. Mol. Biol.* **1977**, *116*, 207–225.
[3] D. G. Drubin, M. W. Kirschner, *J. Cell Biol.* **1986**, *103*, 2739–2746.
[4] R. A. Gonçalves, N. Wijesekara, P. E. Fraser, F. G. De Felice, *Front. Cell. Neurosci.* **2019**, doi: org/10.3389/fncel.2019.00017.
[5] M. Medina, *Int. J. Mol. Sci.* **2018**, *19*, 1160–1173.
[6] J. A. Duce, A. I. Bush, *Prog. Neurobiol.* **2010**, *92*, 1–18.
[7] S. Mondragón-Rodríguez, A. Salas-Gallardo, P. González-Pereyra, M. Macías, B. Ordaz, F. Peña-Ortega, A. Aguilar-Vázquez, E. Orta-Salazar, S. Díaz-Cintra, G. Perry, S. Williams, *J. Biol. Chem.* **2018**, *293*, 8462–8472.
[8] S. Ahmadi, S. Zhu, R. Sharma, D. J. Wilson, H.-B. Kraatz, *J. Inorg. Biochem.* **2019**, *194*, 44–51.
[9] G. Millhauser, *Acc. Chem. Res.* **2004**, *37*, 79–85.
[10] G. Arena, D. La Mendola, G. Pappalardo, I. Sóvágó, E. Rizzarelli, *Coord. Chem. Rev.* **2012**, *256*, 2202–2218.
[11] S. Ayton, P. Lei, A. I. Bush, *Free Radical Biol. Med.* **2013**, *62*, 76–89.
[12] G. Arena, G. Pappalardo, I. Sóvágó, E. Rizzarelli, *Coord. Chem. Rev.* **2012**, *256*, 3–12.
[13] C. Migliorini, E. Porciatti, M. Luczkowski, D. Valensin, *Coord. Chem. Rev.* **2012**, *256*, 352–368.
[14] H. Kozlowski, M. Luczkowski, M. Remelli, D. Valensin, *Coord. Chem. Rev.* **2012**, *256*, 2129–2141.
[15] G. Grasso, S. Bonnet, *Metallomics* **2014**, *6*, 1346–1357.
[16] M. Rowinska-Zyrek, M. Salerno, H. Kozlowski, *Coord. Chem. Rev.* **2015**, *284*, 298–312.
[17] S. S. Leal, H. M. Botelho, C. M. Gomes, *Coord. Chem. Rev.* **2012**, *256*, 2253–2270.
[18] Z.-Y. Mo, Y.-Z. Zhu, H.-L. Zhu, J.-B. Fan, J. Chen, Y. Liang, *J. Biol. Chem.* **2009**, *284*, 34648–34657.
[19] X.-Y. Sun, Y.-P. Wei, Y. Xiong, X.-C. Wang, A.-J. Xie, X.-L. Wang, Y. Yang, Q. Wang, Y.-M Lu, R. Liu, J.-Z. Wang, *J. Biol. Chem.* **2012**, *287*, 11174–11182.
[20] A. Yamamoto, R.-W. Shin, K. Hasegawa, H. Naiki, H. Sato, F. Yoshimasu, T. Kitamoto, *J. Neurochem.* **2002**, *82*, 1137–1147.
[21] L. M. Sayre, G. Perry, P. L. R. Harris, Y. Liu, K. A. Schubert, M. A. Smith, *J. Neurochem.* **2000**, *74*, 270–279.
[22] A. C. Kim, S. Lim, Y. K. Kim, *Int. J. Mol. Sci.* **2018**, *19*, 128–142.
[23] H. Kozlowski, A. Janicka-Klos, P. Stanczak, D. Valensin, G. Valensin, K. Kulon, *Coord. Chem. Rev.* **2008**, *252*, 1069–1078.
[24] I. Sóvágó, K. Várnagy, N. Lihi, Á. Grenács, *Coord. Chem. Rev.* **2016**, *327–328*, 43–54.
[25] Q.-F. Ma, Y.-M. Li, J.-T. Du, K. Kanazawa, T. Nemoto, H. Nakanishi, Y.-F. Zhao, *Biopolymers* **2005**, *79*, 74–85.
[26] L.-X. Zhou, J.-T. Du, Z.-Y. Zeng, W.-H. Wu, Y.-F. Zhao, K. Kanazawa, Y. Ishizuka, T. Nemoto, H. Nakanishi, Y.-M. Li, *Peptides* **2007**, *28*, 2229–2234.
[27] S. Ahmadi, S. Zhu, R. Sharma, B. Wu, R. Soong, R. D. Majumdar, D. J. Wilson, A. J. Simpson, H.-B. Kraatz, *ACS Omega* **2019**, *4*, 5356–5366.
[28] B. Shin, S. Saxena, *J. Phys. Chem. B* **2011**, *115*, 15067–15078.
[29] N. R. Barthélemy, A. Gabelle, C. Hirtz, F. Fenaille, N. Sergeant, S. Schraen-Maschke, J. Vialaret, L. Buée, C. Junot, F. Becher, S. Lehmann, *J. Alzheimer's Dis.* **2016**, *51*, 1033–1043.
[30] G. Di Natale, F. Bellia, M. F. M. Sciacca, T. Campagna, G. Pappalardo, *Inorg. Chim. Acta* **2018**, *472*, 82–92.
[31] G. Di Natale, G. Grasso, G. Impellizzari, D. La Mendola, G. Micera, N. Mihala, Z. Nagy, K. Ősz, G. Pappalardo, V. Rigó, E. Rizzarelli, D. Sanna, I. Sóvágó, *Inorg. Chem.* **2005**, *44*, 7214–7225.
[32] K. Ősz, Z. Nagy, G. Pappalardo, G. Di Natale, D. Sanna, G. Micera, E. Rizzarelli, I. Sóvágó, *Chem. Eur. J.* **2007**, *13*, 7129–7143.
[33] V. Jószai, Z. Nagy, K. Ősz, D. Sanna, G. Di Natale, D. La Mendola, G. Pappalardo, E. Rizzarelli, I. Sóvágó, *J. Inorg. Biochem.* **2006**, *100*, 1399–1409.

© 2019 The Authors. Published by Wiley-VCH Verlag GmbH & Co. KGaA

[34] C. Kállay, K. Várnagy, G. Malandrinos, N. Hadjiliadis, D. Sanna, I. Sóvágó, *Inorg. Chim. Acta* **2009**, *362*, 935–945.
[35] T. Kowalik-Jankowska, M. Ruta-Dolejsz, K. Wiśniewska, L. Łankiewicz, H. Kozłowski, *Dalton Trans.* **2000**, 4511–4519.
[36] R. P. Bonomo, R. Marchelli, G. Tabbì, *J. Inorg. Biochem.* **1995**, *60*, 205–218.
[37] C. Kállay, Z. Nagy, K. Várnagy, G. Malandrinos, N. Hadjiliadis, I. Sóvágó, *Bioinorg. Chem. Appl.* **2007**, 30394–30402.
[38] C. Sánchez-López, L. Rivillas-Acevedo, O. Cruz-Vásgues, L. Quintanar, *Inorg. Chim. Acta* **2018**, *481*, 87–97.
[39] G. Di Natale, I. Turi, G. Pappalardo, I. Sóvágó, E. Rizzarelli, *Chem. Eur. J.* **2015**, *21*, 4071–4084.
[40] D. La Mendola, D. Farkas, F. Bellia, A. Magrì, S. Travaglia, Ö. Hansson, E. Rizzarelli, *Inorg. Chem.* **2012**, *51*, 128–141.
[41] D. Sanna, G. Micera, C. Kállay, V. Rigó, I. Sóvágó, *Dalton Trans.* **2004**, 2702–2707.
[42] S. J. Shields, B. K. Bluhm, D. H. Russell, *J. Am. Soc. Mass Spectrom.* **2000**, *11*, 626–638.
[43] J. A. Loo, P. Hu, R. D. Smith, *J. Am. Soc. Mass Spectrom.* **1994**, *5*, 959–965.
[44] P. Hu, J. A. Loo, *J. Am. Chem. Soc.* **1995**, *117*, 11314–11319.
[45] H. Irving, G. Miles, L. D. Pettit, *Anal. Chim. Acta* **1967**, *38*, 475–488.
[46] L. Zékány, I. Nagypál, in *Computational Methods for the Determination of Formation Constants*, (ed. D. Leggett), Plenum Press, New York **1985**, pp. 291–299.
[47] P. Gans, A. Sabatini, A. Vacca, *J. Chem. Soc., Dalton Trans.* **1985**, 1195–1200.
[48] T. Lund, J. Vanngard, *Chem. Phys.* **1965**, *42*, 2979–2980.
[49] H. R. Gersmann, J. D. Swalen, *J. Chem. Phys.* **1962**, *36*, 3221–3233.
[50] J. R. Pilbrow, M. E. Winfield, *Mol. Phys.* **1973**, *25*, 1073–1092.
[51] M. F. Corrigan, K. S. Murray, B. O. West, J. R. Pilbrow, *Aust. J. Chem.* **1977**, *30*, 2455–2463.

Manuscript received: August 14, 2019
Revised manuscript received: October 19, 2019
Accepted manuscript online: October 26, 2019

© 2019 The Authors. Published by Wiley-VCH Verlag GmbH & Co. KGaA